

RESEARCH ARTICLE

Hippocampal subfield volumes and pre-clinical Alzheimer's disease in 408 cognitively normal adults born in 1946

Thomas D. Parker¹, David M. Cash¹, Christopher A. S. Lane¹, Kirsty Lu¹, Ian B. Malone¹, Jennifer M. Nicholas^{1,2}, Sarah-Naomi James³, Ashvini Keshavan¹, Heidi Murray-Smith¹, Andrew Wong³, Sarah M. Buchanan¹, Sarah E. Keuss¹, Carole H. Sudre^{1,4,5}, Marc Modat^{1,4,5}, David L. Thomas^{6,7}, Sebastian J. Crutch¹, Marcus Richards³, Nick C. Fox¹, Jonathan M. Schott^{1*}

1 The Dementia Research Centre, Queen Square Institute of Neurology, University College London, London, United Kingdom, **2** Department of Medical Statistics, London School of Hygiene and Tropical Medicine, London, United Kingdom, **3** MRC Unit for Lifelong Health and Ageing at University College London, London, United Kingdom, **4** School of Biomedical Engineering and Imaging Sciences, King's College London, London, United Kingdom, **5** Department of Medical Physics and Biomedical Engineering, University College London, London, United Kingdom, **6** Leonard Wolfson Experimental Neurology Centre, Queen Square Institute of Neurology, University College London, London, United Kingdom, **7** Neuroradiological Academic Unit, Department of Brain Repair and Rehabilitation, Queen Square Institute of Neurology, University College London, London, United Kingdom

* j.schott@ucl.ac.uk



OPEN ACCESS

Citation: Parker TD, Cash DM, Lane CAS, Lu K, Malone IB, Nicholas JM, et al. (2019) Hippocampal subfield volumes and pre-clinical Alzheimer's disease in 408 cognitively normal adults born in 1946. *PLoS ONE* 14(10): e0224030. <https://doi.org/10.1371/journal.pone.0224030>

Editor: Yuankai Huo, Vanderbilt University, UNITED STATES

Received: August 1, 2019

Accepted: October 3, 2019

Published: October 17, 2019

Peer Review History: PLOS recognizes the benefits of transparency in the peer review process; therefore, we enable the publication of all of the content of peer review and author responses alongside final, published articles. The editorial history of this article is available here: <https://doi.org/10.1371/journal.pone.0224030>

Copyright: © 2019 Parker et al. This is an open access article distributed under the terms of the [Creative Commons Attribution License](https://creativecommons.org/licenses/by/4.0/), which permits unrestricted use, distribution, and reproduction in any medium, provided the original author and source are credited.

Data Availability Statement: Data cannot be shared publicly in line with data sharing policies specific to the MRC National Survey of Health and Development to protect confidentiality of the study

Abstract

Background

The human hippocampus comprises a number of interconnected histologically and functionally distinct subfields, which may be differentially influenced by cerebral pathology. Automated techniques are now available that estimate hippocampal subfield volumes using *in vivo* structural MRI data. To date, research investigating the influence of cerebral β -amyloid deposition—one of the earliest hypothesised changes in the pathophysiological continuum of Alzheimer's disease—on hippocampal subfield volumes in cognitively normal older individuals, has been limited.

Methods

Using cross-sectional data from 408 cognitively normal individuals born in mainland Britain (age range at time of assessment = 69.2–71.9 years) who underwent cognitive assessment, ¹⁸F-Florbetapir PET and structural MRI on the same 3 Tesla PET/MR unit (spatial resolution 1.1 x 1.1 x 1.1 mm), we investigated the influences of β -amyloid status, age at scan, and global white matter hyperintensity volume on: CA1, CA2/3, CA4, dentate gyrus, presubiculum and subiculum volumes, adjusting for sex and total intracranial volume.

Results

Compared to β -amyloid negative participants (n = 334), β -amyloid positive participants (n = 74) had lower volume of the presubiculum (3.4% smaller, p = 0.012). Despite an age range at scanning of just 2.7 years, older age at time of scanning was associated with lower CA1

participants. Data are available from <https://www.nshd.mrc.ac.uk/data/> for researchers who meet the criteria for access to confidential data.

Funding: This study is principally funded by grants from Alzheimer's Research UK (ARUK-PG2014-1946, ARUK-PG2017-1946), the Medical Research Council Dementias Platform UK (CSUB19166), and the Wolfson Foundation (PR/ylr/18575). The genetic analyses are funded by the Brain Research Trust (UCC14191). Flortetapir amyloid tracer is kindly provided by Avid Radiopharmaceuticals (a wholly owned subsidiary of Eli Lilly) who had no part in the design of the study: we are particularly indebted to the support of the late Dr Chris Clark of Avid Radiopharmaceuticals who championed this study from its outset. The NSHD, MR, and AW are funded by the Medical Research Council (MC_UU_12019/1, MC_UU_12019/2, MC_UU_12019/3). Some researchers are supported by the NIHR Queen Square Dementia BRU (JMS, NCF), UCL Hospitals Biomedical Research Centre (JMS), Leonard Wolfson Experimental Neurology Centre (JMS, NCF). TDP is supported by a Wellcome Trust Clinical Research Fellowship (200109/Z/15/Z). CHS is supported by an Alzheimer's Society Junior Fellowship (AS-JF-17-011). SJC is supported by an Alzheimer's Research UK Senior Research Fellowship. NCF acknowledges support from the MRC, the UK Dementia Research Institute at UCL, and an NIHR Senior Investigator award, and additional funding from the EPSRC. JMS acknowledges the EPSRC (EP/J020990/1), BHF (PG/17/90/33415), Weston Brain Institute (UB170045), and European Union's Horizon 2020 research and innovation programme (Grant 666992).

Competing interests: NCF's research group has received payment for consultancy or for conducting studies from Biogen, Eli Lilly Research Laboratories, GE Healthcare, and Roche. NCF receives no personal compensation for the activities mentioned above. JMS has received research funding from Avid Radiopharmaceuticals (a wholly owned subsidiary of Eli Lilly), has consulted for Roche Pharmaceuticals, Biogen, Merck and Eli Lilly, given educational lectures sponsored by GE Healthcare, Eli Lilly and Biogen, and serves on a Data Safety Monitoring Committee for Axon Neuroscience SE. This does not alter our adherence to PLOS ONE policies on sharing data and materials.

Abbreviations: BaMoS, Bayesian Model Selection; CA, Cornu ammonis; HATA, Hippocampal amygdala transition area; MCI, Mild cognitive impairment; MMSE, Mini mental state examination; MRI, Magnetic Resonance Imaging; NSHD, MRC

($p = 0.007$), CA4 ($p = 0.004$), dentate gyrus ($p = 0.002$), and subiculum ($p = 0.035$) volumes. There was no evidence that white matter hyperintensity volume was associated with any subfield volumes.

Conclusion

These data provide evidence of differential associations in cognitively normal older adults between hippocampal subfield volumes and β -amyloid deposition and, increasing age at time of scan. The relatively selective effect of lower presubiculum volume in the β -amyloid positive group potentially suggest that the presubiculum may be an area of early and relatively specific volume loss in the pathophysiological continuum of Alzheimer's disease. Future work using higher resolution imaging will be key to exploring these findings further.

Introduction

Hippocampal atrophy is a characteristic feature of Alzheimer's disease (AD) and also occurs to a lesser extent in ageing [1–8]. The hippocampus comprises interconnected histologically and functionally distinct subfields and delineation of these subfields from structural magnetic resonance imaging (MRI) has the capacity to provide new insights into mechanisms of disease [9]. There is evidence suggesting hippocampal subfields may be differentially influenced by AD, vascular disease, and ageing [10–25] and have the potential to be more specific biomarkers of neurodegeneration in ageing populations. However, to date, research investigating the relationships between cerebral β -amyloid deposition and the volume of individual hippocampal subfields in cognitively normal older individuals has been limited. In a small sample ($n = 74$), Hsu and colleagues reported β -amyloid associated decreases in not only total hippocampal volume, but also the subiculum and pre-subiculum [26]. The segmentation algorithm utilized in this study has been shown to be vulnerable to mislabelling [27] and there is a requirement for studies with larger sample sizes and more up to date hippocampal subfield segmentation methodology to further investigate this relationship.

We report a cross-sectional analysis of a large sample of individuals all born in mainland Britain in the same week of March 1946 who underwent cognitive assessment, ^{18}F -Flortetapir positron emission tomography (PET) and structural MRI aged 69.2–71.9 years. Utilizing an updated version of Freesurfer's hippocampal subfield segmentation tool based on a computational atlas using *ex vivo*, ultra-high resolution MRI, the objective of this analysis was to investigate the hypothesis that individual hippocampal subfield volumes are differentially associated with β -amyloid deposition, age at time of scan and global white matter hyperintensity volume (WMHV—a surrogate marker of cerebral small vessel disease).

Materials and methods

Participants

Data were analysed from individuals who participated in Insight-46, a neuroscience sub-study of the MRC National Survey of Health and Development (NSHD). The NSHD originally comprised 5362 individuals all born in mainland Britain in one week of March 1946 [28–30]. Insight-46 recruited 502 participants to a single-site study involving detailed clinical and neuropsychological assessment, MRI and ^{18}F -flortetapir PET imaging [31,32] conducted over a 2.7 year period. Ethical approval was granted by the National Research Ethics Service

National Survey of Health and Development; PET, Positron Emission Tomography; SUVR, Standard uptake value ratio; TIV, Total intracranial volume; WMHV, White matter hyperintensity volume.

Committee London (reference 14/LO/1173). All participants provided written informed consent. Exclusions from the analysis were: failure to complete scan ($n = 31$); PET acquisition failure ($n = 8$); failure of WMHV segmentation ($n = 4$); movement artefact felt to impact reliability of hippocampal subfield segmentation ($n = 3$); and participants with evidence of dementia, MCI, major neurological or psychiatric disorder ($n = 48$).

Clinical assessment

As part of Insight-46 Each participant underwent a history of cognitive impairment, major neurological or psychiatric illness. Participant cognitive concern was defined as self-report of memory or cognitive difficulties more than others the same age, or if they felt they would seek medical attention regarding cognitive difficulties. An informant history regarding each participant's cognitive functioning was acquired using the AD8 questionnaire [33,34]. Informant cognitive concern was defined as an AD8 score ≥ 2 .

Cognitive testing included: the Mini-Mental State Examination (MMSE) [35]; the digit-symbol substitution test [36]; logical memory delayed recall [37]; matrix reasoning [38]; and the 12-item Face-Name test [31,39].

Participants were defined as having mild cognitive impairment (MCI) if there was evidence of significant cognitive concerns from the participant or the informant AND objective evidence of an amnesic (sample specific logical memory delayed recall score cut-off ≥ 1.5 standard deviations below the mean) or non-amnesic cognitive deficit (sample specific digit-symbol substitution score cut-off ≥ 1.5 standard deviations below the mean), AND there was no evidence of dementia. Logical memory delayed recall and digit-symbol substitution were selected for this as they both exhibited a normal distribution.

Florbetapir-PET

Concurrent acquisition of PET and MRI was performed on the same Siemens Biograph mMR 3 Tesla PET/MRI scanner. Static PET images representing uptake during a 10-minute period approximately 50 minutes after injection of approximately 370 megabecquerels of ^{18}F -florbetapir were reconstructed using a thoroughly validated pseudo-CT attenuation correction method [40]. The post-uptake images were then rigidly registered to the structural MRI data using a symmetric block matching technique [41]. A previously defined cortical grey matter composite (composed of frontal, temporal, parietal, and cingulate regions [42–46]) was selected as the primary region of interest to assess β -amyloid burden. All voxels in the image were then normalised to a reference region to produce a Standard Uptake Value Ratio (SUVR) image. The reference region selected was a mask of subcortical white matter, eroded one time to avoid partial volume effects. The advantages of the subcortical white matter as a reference region are that it is a relatively uniform tissue type and has less risk of corruption from other tissues compared to other commonly used reference regions (e.g. the cerebellum). Furthermore, SUVR values derived from a white matter reference region have also been shown to correlate better with gold standard arterial sampling based dynamic measurements of tracer uptake compared to SUVR values derived using other widely used reference regions (e.g. the cerebellum)[47]. Gaussian mixture models were used to fit the data and obtain a threshold for β -amyloid positivity. Mixture models with one, two, and three gaussians, were tested, with the best model selected using Bayesian Information Criteria. The best fit for the composite cortical grey matter region of interest was two gaussians. The 99th percentile SUVR value of the Gaussian representing the β -amyloid negative population was selected as the cut-point (0.6104) for β -amyloid positivity,

Structural MRI

MRI sequences included: three-dimensional T1-weighted MPRAGE images (voxel size 1.1x1.1x1.1 mm³ isotropic; TE/TR = 2.92/2000, total time = 5 minutes 6 seconds) and three-dimensional FLAIR images using an IR-SPACE acquisition scheme (voxel size 1.1 x1.1x1.1 mm³ isotropic; TE/TR = 402/5000, total time = 6 minutes 27 seconds) [31].

All MRI data were preprocessed for gradwarp and image inhomogeneity [48,49]. Furthermore, all MRI data underwent a detailed quality control process by trained assessor to ensure there was adequate coverage and absence of motion artefact. T1 scans were also assessed for blurring, image wrap-around and contrast problems, and FLAIR for adequate CSF suppression [31].

Hippocampal subfield segmentation was performed using Freesurfer version 6.0; an algorithm based on a computational atlas using *ex vivo*, ultra-high resolution MRI that segments T1-weighted MRI data to the following subfields: CA1, CA2/3, CA4, fimbria, the hippocampal fissure, presubiculum, subiculum, hippocampal tail, parasubiculum, the molecular and granule cell layers of the dentate gyrus (referred to as the “dentate gyrus” for the remainder of the article), the molecular layer and the hippocampal amygdala transition area (HATA) [9]. Visual inspection of each participant’s hippocampal subfield segmentation and corresponding T1-weighted structural MRI data was performed to ensure each segmentation conformed to the hippocampus and there were no clear and obvious errors. This was performed with the caveat that the precise visualisation of the boundaries that define the distinct hippocampal subfields at the spatial resolution used in this study is challenging [50]. The following regions were excluded prior to the analysis: the hippocampal fissure (a thin CSF layer rather than a hippocampal substructure *per se*), the molecular layer (a thin white matter layer, which is at risk of partial volume effects), the fimbria (small volume white matter region, also at risk of partial volume effect), the parasubiculum and HATA (both of which have volumes <100 μ l and may be more prone to noise), and the hippocampal tail (which is not a histologically distinct region, but instead represents a conglomeration of CA1-4 and dentate gyrus) [9]. The hippocampal subfield segmentation and corresponding T1-weighted structural images for each participant were visually inspected to exclude major errors. For each subfield investigated a total was calculated by summing the left and right hemisphere volumes.

Bayesian Model Selection (BaMoS) [51], an automated segmentation tool that uses T1-weighted and FLAIR MRI data, was used to generate a global estimate of WMHV.

Total intracranial volume (TIV) was calculated from the T1-weighted images using statistical parametric mapping 12 software [52].

Statistical approach

Two-sample t-tests, or where there was a material departure from a normal distribution, Wilcoxon rank sum tests, were used to compare continuous clinical and cognitive characteristics between β -amyloid positive and negative groups. Logistic regression models were used to compare categorical variables between β -amyloid positive and negative groups. Spearman’s correlation coefficients were used to assess unadjusted relationships between age at time of scanning and continuous variables. Wilcoxon rank sum tests were used to test associations between age at scanning and categorical variables.

Linear regression models with robust standard errors were used to test the hypothesis that individual hippocampal subfield volumes (dependent variables) are associated with: β -amyloid status, age at time of scan and global WMHV (predictor variables of interest), with additional adjustment for sex and TIV [52]. Following linear regression analysis, mean differences in subfield volumes between β -amyloid positive and negative participants were expressed as a

percentage of the mean total volume of the respective subfield in the β -amyloid negative population. The β -coefficient for age at scan (i.e. estimated difference in volume per year) was expressed as a percentage of the mean total volume of the respective subfield across the whole sample.

A threshold for statistical significance of $p < 0.05$ was utilized throughout the analysis.

Results

Sample characterisation

As individuals were born in the same week, differences in age within the sample were due to the date of assessment and were therefore narrow: median = 70.7 years; range = 69.2–71.9 years. There were no statistically significant differences between β -amyloid positive and negative individuals in the age, WMHV, sex, TIV, logical memory, digit-symbol substitution scores and the 12-item Face-Name test. Matrix reasoning scores were lower in the β -amyloid positive group compared to the β -amyloid negative group ($p = 0.037$). There was a non-significant trend for lower MMSE scores in the β -amyloid positive group compared to the β -amyloid negative group ($p = 0.063$). As would be expected [53], *APOE* genotype strongly predicted $A\beta$ -status, with $\epsilon 4$ carriers being 5.22 times more likely to be β -amyloid positive. Age at time of scan was not associated with sex, TIV, or performance on any neuropsychological tests. There was evidence of a positive association between older age at time of scan and WMHV ($p = 0.013$) (Table 1).

Influence of β -amyloid deposition

Compared to β -amyloid negative participants ($n = 334$), β -amyloid positive participants ($n = 74$) had lower presubiculum volume (3.4% smaller relative to the mean volume in the β -amyloid negative population, $p = 0.012$) independent of age at time of scan, global WMHV, sex and TIV (Table 2). β -amyloid-associated differences in CA1 (1.3%), CA2/3 (0.4%), CA4 (0.1%), dentate gyrus (0.3%) and subiculum (1.8%) volumes were directionally consistent but not significant (Table 2), while there was evidence of lower total hippocampal volume in the β -amyloid positive participants at trend level of significance only (1.6% smaller $p = 0.075$) (Table 2).

To explore asymmetry, post-hoc analysis examining the left and right hemispheres separately in the presubiculum was performed and revealed similar β -amyloid-associated differences in both the left (3.6% decrease, $p = 0.023$) and right presubiculum (3.3% decrease, $p = 0.02$). To explore whether the association observed between β -amyloid and presubiculum volume was driven by cognitively impaired individuals not captured by the MCI diagnostic criteria used to characterise the sample, a post-hoc regression analysis between presubiculum volume and the 12-item Face-Name test (i.e. a test of episodic memory not used in the diagnostic formulation in this study) was performed. There was no evidence that 12-item Face-Name test performance predicted presubiculum volume ($p = 0.82$), nor was there evidence of an interaction between 12-item Face-Name test performance and β -amyloid status in terms of its effect on presubiculum volume ($p = 0.30$).

Influence of age at time of scanning

Older age at time of scan was associated with smaller volumes of CA1 (1.9%/year, $p = 0.007$), CA4 (1.7%/year, $p = 0.004$), dentate gyrus (2.0%/year, $p = 0.002$), subiculum (1.6%/year, $p = 0.035$) and total hippocampus (1.5%/year, $p = 0.012$) independent of β -amyloid status, global WMHV, sex and TIV. There was a non-significant trend for a negative association in

Table 1. Sample characterisation—unadjusted relationships between clinical, demographic and cognitive outcomes with β -amyloid positivity and age at time of scan.

	β -amyloid negative (n = 334)	β -amyloid positive (n = 74)	β -amyloid negative vs positive	Association with age (n = 408)
Age, years, median (IQR)	70.7 (1.2)	70.7 (1.1)	p = 0.66 ^a	-
Male sex, n (%)	166 (49.7%)	40 (54.1%)	OR 0.84; p = 0.5 ^c	Δ = -0.05; p = 0.48 ^a
MMSE, median (IQR) Maximum score = 30	30 (1)	29 (1)	p = 0.063 ^a	ρ = 0.0065; p = 0.9 ^b
Logical memory score, mean (SD) Maximum score = 25	11.7 (3.6)	11.3 (3.7)	p = 0.33 ^d	ρ = 0.018; p = 0.72 ^b
Digit-symbol substitution score, mean (SD) Maximum score = 93	48.8 (10.1)	46.9 (9.7)	p = 0.14 ^d	ρ = -0.014; p = 0.78 ^b
Matrix reasoning, median (IQR) Maximum score = 32	26 (4)	25 (4)	p = 0.037 ^a	ρ = -0.073; p = 0.14 ^b
12-item Face-Name test, median (IQR) Maximum score = 96	66 (28)	68 (27)	p = 0.29 ^a	ρ = -0.063; p = 0.21 ^b
APOE ϵ 4 carrier, n (%) (missing data: n = 2)	76 (22.9%)	45 (60.8%)	OR 5.22; p < 0.0001 ^c	p = 0.49 ^a
TIV, mls, mean (SD)	1426 (133)	1451 (128)	p = 0.14 ^d	ρ = 0.025; p = 0.61 ^b
WMHV, mls, median (IQR)	2.85 (4.84)	3.30 (4.97)	p = 0.48 ^a	ρ = 0.12; p = 0.013 ^b

^aWilcoxon rank sum test

^bSpearman's rank correlation

^clogistic regression

^dt-test

Δ = mean difference; IQR = interquartile range; MMSE = mini-mental state examination; OR = odds ratio; ρ = Spearman's rho; SD = standard deviation; SUVR = standard uptake value ratio; TIV = total intracranial volume; WMHV = white matter hyperintensity volume (mls).

<https://doi.org/10.1371/journal.pone.0224030.t001>

CA2/3 (1.4%/year, p = 0.086); while presubiculum volume was not significantly associated with age at time of scan (Fig 1 and Table 3).

To explore whether any associations specifically observed between age at time of scan and hippocampal subfield volumes might be explained by bias in recruitment order, analyses incorporating a wider range of co-variates that had been shown to predict recruitment in previous Insight-46 analyses (socioeconomic position, educational attainment, and childhood cognitive ability [32]) were also performed and made no material difference to the statistically significant results obtained (Table 4).

Socioeconomic position dichotomized into manual or non-manual based on occupation at 53 years (or earlier if missing) [56]

Influence of WMHV

There was no evidence that WMHV predicted any hippocampal subfield volumes (Table 3).

Discussion

Few studies have explored the extent to which cerebral β -amyloid deposition are associated with hippocampal subfield volume in cognitively normal older adults. In a large sample of

Table 2. Independent influence of amyloid positivity on individual hippocampal subfield volumes in cognitively normal Insight-46 participants (n = 408) using linear regression models with robust standard errors (co- variates = age at scan, WMHV, sex and TIV).

	β -amyloid negative (n = 334)	β -amyloid positive (n = 74)	Absolute mean difference between β -amyloid negative and positive (95% CI)	%mean difference between β -amyloid negative and positive	p
CA1	1196 (141)	1195 (111)	-15.4 (-38.6, 7.9)	1.3%	0.19
CA2/3	406 (53)	410 (47)	-1.5 (-12.3, 9.3)	0.4%	0.78
CA4	482 (50)	487 (44)	-0.6 (-10.4, 9.3)	0.1%	0.91
Dentate gyrus	554 (60)	558 (53)	-1.8 (-13.5, 10.0)	0.3%	0.77
Presubiculum	582 (68)	568 (67)	-19.9 (-35.4, -4.5)	3.4%	0.012*
Subiculum	832 (100)	827 (86)	-15.0 (-34.4, 4.5)	1.8%	0.13
Total volume	6515 (659)	6487 (526)	-101.3 (-213.0, 10.3)	1.6%	0.075

CA = Cornu ammonis; TIV = total intracranial volume; WMHV = white matter hyperintensity volume

*p<0.05

<https://doi.org/10.1371/journal.pone.0224030.t002>

cognitively normal older individuals aged 69.2–71.9 years, we show differential associations between hippocampal subfield volumes β -amyloid deposition, and age at time of scan.

β -amyloid positive individuals had lower presubiculum volumes compared to β -amyloid negative individuals. Importantly, this was independent of age, sex, TIV and WMHV (a surrogate marker of cerebral small vessel disease [51]).

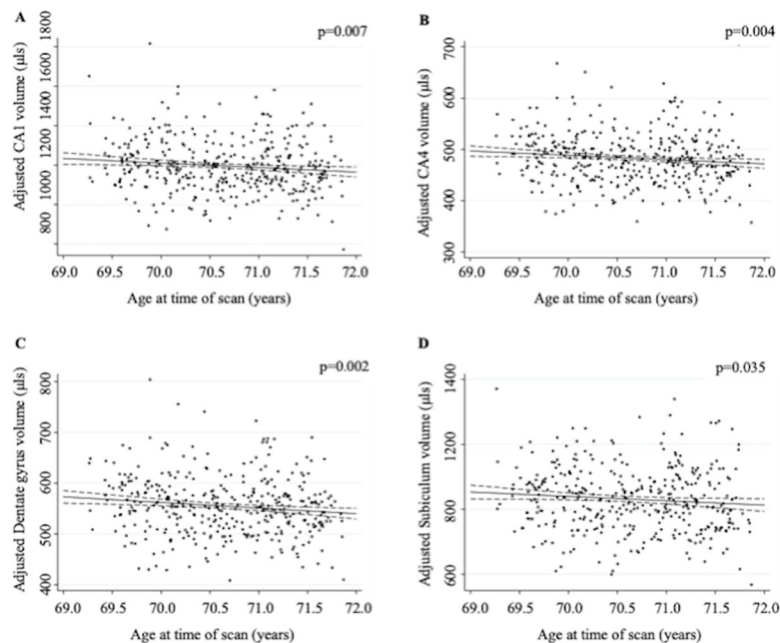


Fig 1. Age is associated with lower CA1 (panel A), CA4 (panel B), dentate gyrus (panel C) and subiculum (panel D) volume in cognitively normal older adults following adjustment for sex, TIV, amyloid status and WMHV. Dashed lines represent 95% confidence intervals, TIV = total intracranial volume; WMHV = white matter hyperintensity volume.

<https://doi.org/10.1371/journal.pone.0224030.g001>

Table 3. Independent influence of age at time of scan and WMHV on individual hippocampal subfield volumes in cognitively normal Insight-46 participants (n = 408) using linear regression models with robust standard errors (co- variates = β -amyloid status, sex and TIV). Unstandardised β -coefficient for age represents mean subfield volume difference in μ l per year. Unstandardised β -coefficient for WMHV represents mean subfield volume difference in μ l per ml of WMHV.

	Total volume, μ l (SD)	Increasing age at time of scan (μ l/year)		% difference in volume per one year of age	WMHV (μ l/ml)	
		β -coefficient (95% CI)	p		β -coefficient (95% CI)	p
CA1	1196 (136)	-23.0 (-39.8, -6.3)	0.007*	1.9%	-0.59 (-2.35, 1.17)	0.51
CA2/3	407 (52)	-5.7 (-12.1, 0.8)	0.086	1.4%	0.06 (-0.62, 0.74)	0.86
CA4	483 (49)	-8.4 (-14.0, -2.7)	0.004*	1.7%	-0.13 (-0.8, 0.54)	0.7
Dentate gyrus	555 (59)	-11.1 (-17.9, -4.2)	0.002*	2.0%	-0.35 (-1.17, 0.47)	0.4
Presubiculum	580 (68)	-5.9 (-14.6, 2.8)	0.18	1.0%	-0.2 (-1.24, 0.84)	0.71
Subiculum	831 (98)	-13.5 (-25.9, -1.0)	0.035*	1.6%	-0.7 (-2.17, 0.77)	0.35
Tail	1047 (133)	-4.9 (-23.9, 14.1)	0.61	1.5%	-0.07 (-2.21, 2.21)	0.95
Total volume	6510 (637)	-99.6 (-176.9, -22.3)	0.012*	1.9%	-3.13 (-11.67, 5.42)	0.47

CA = Cornu ammonis; TIV = total intracranial volume; WHMV = white matter hyperintensity volume

*p<0.05

<https://doi.org/10.1371/journal.pone.0224030.t003>

Table 4. Additional adjustment for wide range of potential confounders that could be related to recruitment order makes no material difference to associations observed between hippocampal subfield volumes and age at time of scan.

	Increasing age (μ l/year) Co-variates = sex, TIV, β -amyloid status, and WMHV		Increasing age (μ l/year) Co-variates = sex, TIV, β -amyloid status, WMHV, socioeconomic position, education, childhood cognition	
	β -coefficient (95% CI)	p	β -coefficient (95% CI)	p
CA1	-23.0 (-39.8, -6.3)	0.007*	-23.1 (-40.0, -6.2)	0.008*
CA2/3	-5.7 (-12.1, 0.8)	0.086	-6.0 (-12.5, 0.6)	0.074
CA4	-8.4 (-14.0, -2.7)	0.004*	-8.7 (-14.4, -3.0)	0.003*
Dentate gyrus	-11.1 (-17.9, -4.2)	0.002*	-11.2 (-18.2, -4.4)	0.001*
Presubiculum	-5.9 (-14.6, 2.8)	0.18	-6.4 (-15.1, 2.2)	0.15
Subiculum	-13.5 (-25.9, -1.0)	0.035*	-13.8 (-26.3-1.4)	0.03*
Total volume	-99.6 (-176.9, -22.3)	0.012*	-99.1 (-176.1, -22.2)	0.012*

CA = Cornu ammonis; TIV = total intracranial volume; WHMV = white matter hyperintensity volume

*p<0.05. Childhood cognitive function was measured at age 8 (or age 11 or 15 if this was missing) as the sum of scores of four tests of verbal and non-verbal ability standardised into a z-score [54]. Educational attainment was dichotomized into those with advanced (e.g. 'A level') or higher (e.g. university) qualifications, versus those below this level [55].

<https://doi.org/10.1371/journal.pone.0224030.t004>

Research into hippocampal subfield volumes in pre-clinical populations previously has been limited. Hsu and colleagues reported β -amyloid associated decreases in the subiculum and pre-subiculum in a small sample of cognitively normal individuals ($n = 74$) [26], the pattern of which is broadly consistent with the findings presented in this analysis. However, the magnitude of these volume differences was much greater (approximately 10–12% compared to 3–4% in Insight 46). A number of factors including smaller sample size and wide age range (with a trend for the β -amyloid positive to be older) as well recruitment via convenience sampling in the previous study may account for these discrepancies. Furthermore, Hsu and colleagues utilized a previous version of Freesurfer's hippocampal subfield segmentation algorithm, which has been shown to be vulnerable to mislabelling [27].

Although studies across the pathophysiological continuum of AD suggest that atrophy of the presubiculum may be one of the earliest hippocampal anatomical markers of AD [15,20], no other studies to date, have demonstrated lower presubiculum volumes in relative isolation in β -amyloid positive cognitively normal individuals. Although the effect size was small, it was consistent across cerebral hemispheres suggesting both that this is a symmetrical effect, and also is unlikely to be the result of a type I error.

Although there was a trend for lower total hippocampal volume in our study, this did not attain a 5% level of significance. Previous cross-sectional studies focusing on total hippocampal volume alone have reported evidence of reduced baseline hippocampal volume associated with cerebral β -amyloid deposition in cognitively normal older individuals [20,57–62], whereas others have not [63,64]. Many studies reporting detectable differences in hippocampal volume include participants who are much older than the age range tested in this study and consequently are likely to be further along the pathophysiological continuum of AD and to have undergone greater levels of neuronal loss. Our data potentially suggest that individual hippocampal subfields may decrease in volume at an earlier stage of the pathophysiological continuum of AD before significant total hippocampal volume loss is detectable.

We also found that several different hippocampal regions—namely CA1, CA4, dentate gyrus and the subiculum—had a negative association with increasing age at time of scan. Previous work using a range of techniques has identified similar findings with age-associated volume loss in CA1 and the dentate gyrus [65]; CA1, dentate gyrus and CA4 [18]; subiculum and dentate gyrus [66]; CA1 and CA2 [67]. In addition to biological ageing effects, it is also possible that the age-related observations in this study might reflect differences in the characteristics of participants based on the order of recruitment. However, supplementary analyses incorporating a wide range of confounders that may influence study recruitment [32] made no difference to the associations observed between hippocampal subfield volumes and age at time of scan. It is unlikely technical factors (e.g. scanner drift), would explain the results given the lack of a relationship between age at time of scan and TIV (a morphometric measurement that would be expected to stay relatively stable across the age range studied). Additionally, the magnitude of the association between hippocampal subfields and age at time of scan were not dissimilar to estimated rates of change in hippocampal volume derived from studies where healthy older adults have been scanned multiple times over a short time interval [8].

Notably, the presubiculum was not associated with age at time of scan, even at a trend level, suggesting the β -amyloid associated effect of lower presubiculum volume observed in the β -amyloid positive group is unlikely to be related to ageing effects. Furthermore, neuropathological data suggests that the presubiculum is a site of large, evenly distributed “lake-like” β -amyloid deposits [68,69] in AD, but devoid of neurofibrillary tau deposition [69,70]. This might explain both the relatively selective β -amyloid associated volume difference in the presubiculum, as well as the relative sparing of an association with age at time of scan which has been

hypothesised to underpinned by primary age-related tauopathy a process thought to be independent of β -amyloid deposition [71,72].

Previous studies have shown that WMHV and cerebrovascular disease are important determinants of hippocampal atrophy in older adults [22,73]. However, we found no evidence that WMHV was associated with hippocampal subfield volumes. This may suggest that, at least in cognitively normal individuals aged approximately 70 years old, vascular disease burden as estimated by WMHV does not significantly influence cross-sectional hippocampal volume.

One significant limitation of this study is the spatial resolution (1.1 mm x 1.1 mm x 1.1 mm) provided by the volumetric structural T1-weighted MRI acquisition protocol utilized, as at this resolution boundaries important for subfield demarcation are not entirely visible and the computational atlas based on high resolution *ex vivo* data, relies on prior encoded information to provide volumetric estimates of individual hippocampal subfields [9]. It is clear that higher resolution imaging studies [14,18,74,75] are an important area of research. In particular, large scale comparison of results from hippocampal subfield segmentation protocols derived from widely used image acquisition protocols, such as the ones provided by this study, with higher resolution, but less widely implemented, imaging protocols are required. Another limitation of the study is the lack of a biomarker of neurofibrillary tangle deposition. A recent study of 88 individuals with a family history of AD investigating hippocampal sub-region volumes found those with abnormal CSF β -amyloid, but normal CSF tau had increased right subiculum volumes, whilst abnormal CSF β -amyloid and abnormal CSF tau was associated with decreased right subiculum volume [21] suggesting the presence of tau deposition is important for hippocampal atrophy and has selective effects on certain subfields. Future studies of hippocampal subfields employing tau PET imaging [76,77] will be of interest, particularly as tau is likely to influence hippocampal structure in both an β -amyloid dependent [77] and independent manner [71,72]. In addition, formal correction for multiple comparisons was not performed in this analysis, although efforts were made to constrain the analysis to total subfield volumes (sum of left and right) in the first instance and excluded subfields that were likely to be unreliable. Furthermore, to what extent hippocampal subfields are truly independent, and therefore to what extent it is valid to apply such techniques is unclear [16]. Finally, the cross-sectional nature of this study is a further limitation and confirmation with longitudinal data, including investigation of how hippocampal subfield volumes associate with changes on neuropsychological testing performance over time, will be required [78].

In summary, we present evidence for differential associations between hippocampal subfield volumes and β -amyloid deposition and, increasing age at time of scan and highlight the potential for hippocampal subfield volumes to provide insights into ageing and preclinical AD. Future work focusing on hippocampal subfield morphometry, particularly utilising higher resolution imaging is an important area of future research.

Acknowledgments

We are very grateful to those study members who helped in the design of the study through focus groups, and to the participants both for their contributions to Insight 46 and for their commitments to research over the last seven decades. We are grateful to the radiographers and nuclear medicine physicians at the UCL Institute of Nuclear Medicine, and to the staff at the Leonard Wolfson Experimental Neurology Centre at UCL. This study is principally funded by grants from Alzheimer's Research UK (ARUK-PG2014-1946, ARUK-PG2017-1946), the Medical Research Council Dementias Platform UK (CSUB19166), and the Wolfson Foundation (PR/ylr/18575). The genetic analyses are funded by the Brain Research Trust (UCC14191). Flortbetapir amyloid tracer is kindly provided by Avid Radiopharmaceuticals (a wholly owned

subsidiary of Eli Lilly) who had no part in the design of the study: we are particularly indebted to the support of the late Dr Chris Clark of Avid Radiopharmaceuticals who championed this study from its outset. The NSHD, MR, RH and AW are funded by the Medical Research Council (MC_UU_12019/1, MC_UU_12019/2, MC_UU_12019/3). Some researchers are supported by the NIHR Queen Square Dementia BRU (JMS, NCF), UCL Hospitals Biomedical Research Centre (JMS), Leonard Wolfson Experimental Neurology Centre (JMS, NCF). TDP is supported by a Wellcome Trust Clinical Research Fellowship (200109/Z/15/Z). CHS is supported by an Alzheimer's Society Junior Fellowship (AS-JF-17-011). SJC is supported by an Alzheimer's Research UK Senior Research Fellowship. NCF acknowledges support from the MRC, the UK Dementia Research Institute at UCL, and an NIHR Senior Investigator award, and additional funding from the EPSRC. JMS acknowledges the EPSRC (EP/J020990/1), BHF (PG/17/90/33415), Weston Brain Institute (UB170045), and European Union's Horizon 2020 research and innovation programme (Grant 666992).

Author Contributions

Conceptualization: Thomas D. Parker, Marcus Richards, Nick C. Fox, Jonathan M. Schott.

Data curation: Christopher A. S. Lane, Kirsty Lu, Ian B. Malone, Sarah M. Buchanan, Sarah E. Keuss.

Formal analysis: Thomas D. Parker, David M. Cash, Jennifer M. Nicholas.

Funding acquisition: Thomas D. Parker.

Investigation: Christopher A. S. Lane, Kirsty Lu, Sarah-Naomi James, Ashvini Keshavan.

Methodology: Thomas D. Parker, David M. Cash, Christopher A. S. Lane, Kirsty Lu, Ian B. Malone, Jennifer M. Nicholas, Sarah-Naomi James, Andrew Wong, Sarah E. Keuss, Carole H. Sudre, Marc Modat, David L. Thomas, Sebastian J. Crutch.

Project administration: Heidi Murray-Smith, Andrew Wong, Sarah M. Buchanan, Sarah E. Keuss.

Software: Marc Modat.

Writing – original draft: Thomas D. Parker.

Writing – review & editing: Thomas D. Parker, David M. Cash, Christopher A. S. Lane, Kirsty Lu, Ian B. Malone, Jennifer M. Nicholas, Sarah-Naomi James, Ashvini Keshavan, Heidi Murray-Smith, Andrew Wong, Sarah M. Buchanan, Sarah E. Keuss, Carole H. Sudre, David L. Thomas, Sebastian J. Crutch, Marcus Richards, Nick C. Fox, Jonathan M. Schott.

References

1. Seab JP, Jagust WJ, Wong ST, Roos MS, Reed BR, Budinger TF. Quantitative NMR measurements of hippocampal atrophy in Alzheimer's disease. *Magn Reson Med*. 1988 Oct; 8(2):200–8. <https://doi.org/10.1002/mrm.1910080210> PMID: 3210957
2. Kesslak JP, Nalcioglu O, Cotman CW. Quantification of magnetic resonance scans for hippocampal and parahippocampal atrophy in Alzheimer's disease. *Neurology*. 1991 Jan; 41(1):51–4. <https://doi.org/10.1212/wnl.41.1.51> PMID: 1985296
3. Jack CR, Petersen RC, O'Brien PC, Tangalos EG. MR-based hippocampal volumetry in the diagnosis of Alzheimer's disease. *Neurology*. 1992 Jan; 42(1):183–8. <https://doi.org/10.1212/wnl.42.1.183> PMID: 1734300
4. Scheltens P, Leys D, Barkhof F, Huglo D, Weinstein HC, Vermersch P, et al. Atrophy of medial temporal lobes on MRI in "probable" Alzheimer's disease and normal ageing: diagnostic value and neuropsychological correlates. *J Neurol Neurosurg Psychiatry*. 1992 Oct; 55(10):967–72.

5. Jack CR, Petersen RC, Xu Y, O'Brien PC, Smith GE, Ivnik RJ, et al. Rates of hippocampal atrophy correlate with change in clinical status in aging and AD. *Neurology*. 2000 Aug 22; 55(4):484–9. <https://doi.org/10.1212/wnl.55.4.484> PMID: 10953178
6. Bobinski M, de Leon MJ, Wegiel J, Desanti S, Convit A, Saint Louis LA, et al. The histological validation of post mortem magnetic resonance imaging-determined hippocampal volume in Alzheimer's disease. *Neuroscience*. 2000; 95(3):721–5. [https://doi.org/10.1016/s0306-4522\(99\)00476-5](https://doi.org/10.1016/s0306-4522(99)00476-5) PMID: 10670438
7. Jack CR, Dickson DW, Parisi JE, Xu YC, Cha RH, O'Brien PC, et al. Antemortem MRI findings correlate with hippocampal neuropathology in typical aging and dementia. *Neurology*. 2002 Mar 12; 58(5):750–7. <https://doi.org/10.1212/wnl.58.5.750> PMID: 11889239
8. Cash DM, Frost C, Iheme LO, Ünay D, Kandemir M, Fripp J, et al. Assessing atrophy measurement techniques in dementia: Results from the MIRIAD atrophy challenge. *Neuroimage*. 2015 Dec; 123:149–64. <https://doi.org/10.1016/j.neuroimage.2015.07.087> PMID: 26275383
9. Iglesias JE, Augustinack JC, Nguyen K, Player CM, Player A, Wright M, et al. A computational atlas of the hippocampal formation using ex vivo, ultra-high resolution MRI: Application to adaptive segmentation of in vivo MRI. *Neuroimage*. 2015 Jul 15; 115:117–37. <https://doi.org/10.1016/j.neuroimage.2015.04.042> PMID: 25936807
10. Apostolova LG, Mosconi L, Thompson PM, Green AE, Hwang KS, Ramirez A, et al. Subregional hippocampal atrophy predicts Alzheimer's dementia in the cognitively normal. *Neurobiol Aging*. 2010 Jul; 31(7):1077–88. <https://doi.org/10.1016/j.neurobiolaging.2008.08.008> PMID: 18814937
11. Mueller SG, Schuff N, Yaffe K, Madison C, Miller B, Weiner MW. Hippocampal atrophy patterns in mild cognitive impairment and Alzheimer's disease. *Hum Brain Mapp*. 2010 Sep; 31(9):1339–47. <https://doi.org/10.1002/hbm.20934> PMID: 20839293
12. La Joie R, Perrotin A, De La Sayette V, Egret S, Dœuvre L, Belliard S, et al. Hippocampal subfield volumetry in mild cognitive impairment, Alzheimer's disease and semantic dementia. *NeuroImage Clin*. 2013; 3:155–62. <https://doi.org/10.1016/j.nicl.2013.08.007> PMID: 24179859
13. Pini L, Pievani M, Bocchetta M, Altomare D, Bosco P, Cavado E, et al. Brain atrophy in Alzheimer's Disease and aging. *Ageing Res Rev*. 2016; 30:25–48. <https://doi.org/10.1016/j.arr.2016.01.002> PMID: 26827786
14. Blanken AE, Hurtz S, Zarow C, Biado K, Honarpisheh H, Somme J, et al. Associations between hippocampal morphometry and neuropathologic markers of Alzheimer's disease using 7 T MRI. *NeuroImage Clin*. 2017; 15:56–61. <https://doi.org/10.1016/j.nicl.2017.04.020> PMID: 28491492
15. Carlesimo GA, Piras F, Orfei MD, Iorio M, Caltagirone C, Spalletta G. Atrophy of presubiculum and subiculum is the earliest hippocampal anatomical marker of Alzheimer's disease. *Alzheimer's Dement (Amsterdam, Netherlands)*. 2015 Mar; 1(1):24–32.
16. Mak E, Gabel S, Su L, Williams GB, Arnold R, Passamonti L, et al. Multi-modal MRI investigation of volumetric and microstructural changes in the hippocampus and its subfields in mild cognitive impairment, Alzheimer's disease, and dementia with Lewy bodies. *Int psychogeriatrics*. 2017; 29(4):545–55.
17. Apostolova LG, Dutton RA, Dinov ID, Hayashi KM, Toga AW, Cummings JL, et al. Conversion of Mild Cognitive Impairment to Alzheimer Disease Predicted by Hippocampal Atrophy Maps. *Arch Neurol*. 2006 May 1; 63(5):693. <https://doi.org/10.1001/archneur.63.5.693> PMID: 16682538
18. Wisse LEM, Biessels GJ, Heringa SM, Kuijf HJ, Koek DL, Luijten PR, et al. Hippocampal subfield volumes at 7T in early Alzheimer's disease and normal aging. *Neurobiol Aging*. 2014;
19. Small SA, Schobel SA, Buxton RB, Witter MP, Barnes CA. A pathophysiological framework of hippocampal dysfunction in ageing and disease. *Nat Rev Neurosci*. 2011 Oct 7; 12(10):585–601. <https://doi.org/10.1038/nrn3085> PMID: 21897434
20. Hsu PJ, Shou H, Benzinger T, Marcus D, Durbin T, Morris JC, et al. Amyloid burden in cognitively normal elderly is associated with preferential hippocampal subfield volume loss. *J Alzheimers Dis*. 2015; 45(1):27–33. <https://doi.org/10.3233/JAD-141743> PMID: 25428255
21. Tardif CL, Devenyi GA, Amaral RSC, Pelleieux S, Poirier J, Rosa-Neto P, et al. Regionally specific changes in the hippocampal circuitry accompany progression of cerebrospinal fluid biomarkers in pre-clinical Alzheimer's disease. *Hum Brain Mapp*. 2018 Nov 21;
22. Wu W, Brickman AM, Luchsinger J, Ferrazzano P, Pichiule P, Yoshita M, et al. The brain in the age of old: the hippocampal formation is targeted differentially by diseases of late life. *Ann Neurol*. 2008 Dec; 64(6):698–706. <https://doi.org/10.1002/ana.21557> PMID: 19107993
23. de Flores R, La Joie R, Chételat G. Structural imaging of hippocampal subfields in healthy aging and Alzheimer's disease. *Neuroscience*. 2015.
24. Shing YL, Rodrigue KM, Kennedy KM, Fandakova Y, Bodammer N, Werkle-Bergner M, et al. Hippocampal subfield volumes: Age, vascular risk, and correlation with associative memory. *Front Aging Neurosci*. 2011;

25. Bender AR, Daugherty AM, Raz N. Vascular risk moderates associations between hippocampal subfield volumes and memory. *J Cogn Neurosci*. 2013;
26. Hsu PJ, Shou H, Benzinger T, Marcus D, Durbin T, Morris JC, et al. Amyloid burden in cognitively normal elderly is associated with preferential hippocampal subfield volume loss. *J Alzheimer's Dis*. 2015; 45(1):27–33.
27. Wisse LEM, Biessels GJ, Geerlings MI. A Critical Appraisal of the Hippocampal Subfield Segmentation Package in FreeSurfer. *Front Aging Neurosci*. 2014; 6:261. <https://doi.org/10.3389/fnagi.2014.00261> PMID: 25309437
28. Stafford M, Black S, Shah I, Hardy R, Pierce M, Richards M, et al. Using a birth cohort to study ageing: representativeness and response rates in the National Survey of Health and Development. *Eur J Ageing*. 2013; 10(2):145–57. <https://doi.org/10.1007/s10433-013-0258-8> PMID: 23637643
29. Kuh D, Wong A, Shah I, Moore A, Popham M, Curran P, et al. The MRC National Survey of Health and Development reaches age 70: maintaining participation at older ages in a birth cohort study. *Eur J Epidemiol*. 2016 Nov; 31(11):1135–47. <https://doi.org/10.1007/s10654-016-0217-8> PMID: 27995394
30. Wadsworth M, Kuh D, Richards M, Hardy R. Cohort profile: The 1946 National Birth Cohort (MRC National Survey of Health and Development). *Int J Epidemiol*. 2006; 35(1):49–54. <https://doi.org/10.1093/ije/dyi201> PMID: 16204333
31. Lane CA, Parker TD, Cash DM, Macpherson K, Donnachie E, Murray-Smith H, et al. Study protocol: Insight 46—a neuroscience sub-study of the MRC National Survey of Health and Development. *BMC Neurol*. 2017 Dec 18; 17(1):75. <https://doi.org/10.1186/s12883-017-0846-x> PMID: 28420323
32. James S-N, Lane CA, Parker TD, Lu K, Collins JD, Murray-Smith H, et al. Using a birth cohort to study brain health and preclinical dementia: Recruitment and participation rates in Insight 46. *BMC Res Notes*. 2018;11(1).
33. Galvin JE, Roe CM, Powlishta KK, Coats MA, Muich SJ, Grant E, et al. The AD8: a brief informant interview to detect dementia. *Neurology*. 2005 Aug 23; 65(4):559–64. <https://doi.org/10.1212/01.wnl.0000172958.95282.2a> PMID: 16116116
34. Galvin JE, Roe CM, Xiong C, Morris JC. Validity and reliability of the AD8 informant interview in dementia. *Neurology*. 2006 Dec 12; 67(11):1942–8. <https://doi.org/10.1212/01.wnl.0000247042.15547.eb> PMID: 17159098
35. Folstein MF, Folstein SE, McHugh PR. "Mini-mental state." *J Psychiatr Res*. 1975 Nov; 12(3):189–98. [https://doi.org/10.1016/0022-3956\(75\)90026-6](https://doi.org/10.1016/0022-3956(75)90026-6) PMID: 1202204
36. Wechsler D. Wechsler Adult Intelligence Scale—Revised. 1981.
37. Wechsler D. Wechsler Memory Scale—Revised Edition. 1987.
38. Wechsler D. The Wechsler abbreviated scale of intelligence. San Antonio, TX: The Psychological Corporation; 1999.
39. Papp K V, Amariglio RE, Dekhtyar M, Roy K, Wigman S, Bamfo R, et al. Development of a psychometrically equivalent short form of the Face-Name Associative Memory Exam for use along the early Alzheimer's disease trajectory. *Clin Neuropsychol*. 2014/05/13. 2014; 28(5):771–85. <https://doi.org/10.1080/13854046.2014.911351> PMID: 24815535
40. Burgos N, Cardoso MJ, Thielemans K, Modat M, Dickson J, Schott JM, et al. Multi-contrast attenuation map synthesis for PET/MR scanners: assessment on FDG and Flortbetapir PET tracers. *Eur J Nucl Med Mol Imaging*. 2015 Aug; 42(9):1447–58. <https://doi.org/10.1007/s00259-015-3082-x> PMID: 26105119
41. Modat M, Cash DM, Daga P, Winston GP, Duncan JS, Ourselin S. Global image registration using a symmetric block-matching approach. *J Med Imaging*. 2014 Sep 19; 1(2):24003-1–24003-6.
42. Fleisher AS, Chen K, Liu X, Roontiva A, Thiyyagura P, Ayutyanont N, et al. Using positron emission tomography and flortbetapir F18 to image cortical amyloid in patients with mild cognitive impairment or dementia due to Alzheimer disease. *Arch Neurol*. 2011;
43. Landau SM, Marks SM, Mormino EC, Rabinovici GD, Oh H, O'Neil JP, et al. Association of lifetime cognitive engagement and low β -amyloid deposition. *Arch Neurol*. 2012;
44. Landau SM, Fero A, Baker SL, Koeppe R, Mintun M, Chen K, et al. Measurement of Longitudinal -Amyloid Change with 18F-Flortbetapir PET and Standardized Uptake Value Ratios. *J Nucl Med*. 2015;
45. Landau SM, Breault C, Joshi AD, Pontecorvo M, Mathis CA, Jagust WJ, et al. Amyloid- Imaging with Pittsburgh Compound B and Flortbetapir: Comparing Radiotracers and Quantification Methods. *J Nucl Med*. 2013;
46. Egan MF, Kost J, Tariot PN, Aisen PS, Cummings JL, Vellas B, et al. Randomized Trial of Verubecestat for Mild-to-Moderate Alzheimer's Disease. *N Engl J Med*. 2018 May 3; 378(18):1691–703. <https://doi.org/10.1056/NEJMoa1706441> PMID: 29719179

47. Ottoy J, Verhaeghe J, Niemantsverdriet E, Wyffels L, Somers C, De Roeck E, et al. Validation of the Semiquantitative Static SUVR Method for 18 F-AV45 PET by Pharmacokinetic Modeling with an Arterial Input Function. *J Nucl Med*. 2017;
48. Jovicich J, Czanner S, Greve D, Haley E, van der Kouwe A, Gollub R, et al. Reliability in multi-site structural MRI studies: effects of gradient non-linearity correction on phantom and human data. *Neuroimage*. 2006 Apr; 30(2):436–43. <https://doi.org/10.1016/j.neuroimage.2005.09.046> PMID: 16300968
49. Tustison NJ, Avants BB, Cook PA, Zheng Y, Egan A, Yushkevich PA, et al. N4ITK: improved N3 bias correction. *IEEE Trans Med Imaging*. 2010 Jun; 29(6):1310–20. <https://doi.org/10.1109/TMI.2010.2046908> PMID: 20378467
50. Parker TD, Slattery CF, Yong KXX, Nicholas JM, Paterson RW, Foulkes AJM, et al. Differences in hippocampal subfield volume are seen in phenotypic variants of early onset Alzheimer's disease. *NeuroImage Clin*. 2018;
51. Sudre CH, Cardoso MJ, Bouvy WH, Biessels GJ, Barnes J, Ourselin S. Bayesian Model Selection for Pathological Neuroimaging Data Applied to White Matter Lesion Segmentation. *IEEE Trans Med Imaging*. 2015;
52. Malone IB, Leung KK, Clegg S, Barnes J, Whitwell JL, Ashburner J, et al. Accurate automatic estimation of total intracranial volume: a nuisance variable with less nuisance. *Neuroimage*. 2015 Jan 1; 104:366–72. <https://doi.org/10.1016/j.neuroimage.2014.09.034> PMID: 25255942
53. Jansen WJ, Ossenkoppele R, Knol DL, Tijms BM, Scheltens P, Verhey FRJ, et al. Prevalence of Cerebral Amyloid Pathology in Persons Without Dementia: A Meta-analysis. *JAMA*. 2015 May 19; 313(19):1924–38. <https://doi.org/10.1001/jama.2015.4668> PMID: 25988462
54. Pigeon D. Tests used in the 1954 and 1957 surveys. Douglas J, editor. In the Home and the School (Appendix 1). Macgibbon & Kee; 1964.
55. Department of Education and Science. Burnham further education committee grading courses. London; 1972.
56. Guralnik JM, Butterworth S, Wadsworth MEJ, Kuh D. Childhood socioeconomic status predicts physical functioning a half century later. *J Gerontol A Biol Sci Med Sci*. 2006;
57. Mormino EC, Kluth JT, Madison CM, Rabinovici GD, Baker SL, Miller BL, et al. Episodic memory loss is related to hippocampal-mediated β -amyloid deposition in elderly subjects. *Brain*. 2008; 132(5):1310–23.
58. Storandt M, Mintun M a, Head D, Morris JC. Cognitive decline and brain volume loss as signatures of cerebral amyloid-beta peptide deposition identified with Pittsburgh compound B: cognitive decline associated with Abeta deposition. *Arch Neurol*. 2009; 66(12):1476–81. <https://doi.org/10.1001/archneurol.2009.272> PMID: 20008651
59. Bourgeat P, Ch etelat G, Villemagne VL, Fripp J, Raniga P, Pike K, et al. β -Amyloid burden in the temporal neocortex is related to hippocampal atrophy in elderly subjects without dementia. *Neurology*. 2010; 74(2):121–7. <https://doi.org/10.1212/WNL.0b013e3181c918b5> PMID: 20065247
60. Dor e V, Villemagne VL, Bourgeat P, Fripp J, Acosta O, Chet elat G, et al. Cross-sectional and longitudinal analysis of the relationship between A β deposition, cortical thickness, and memory in cognitively unimpaired individuals and in Alzheimer disease. *JAMA Neurol*. 2013; 70(7):903–11. <https://doi.org/10.1001/jamaneurol.2013.1062> PMID: 23712469
61. Petersen RC, Wiste HJ, Weigand SD, Rocca WA, Roberts RO, Mielke MM, et al. Association of Elevated Amyloid Levels With Cognition and Biomarkers in Cognitively Normal People From the Community. *JAMA Neurol*. 2016 Jan; 73(1):85–92. <https://doi.org/10.1001/jamaneurol.2015.3098> PMID: 26595683
62. Dubois B, Epelbaum S, Nyasse F, Bakardjian H, Gagliardi G, Uspenskaya O, et al. Cognitive and neuroimaging features and brain β -amyloidosis in individuals at risk of Alzheimer's disease (INSIGHT-preAD): a longitudinal observational study. *Lancet Neurol*. 2018 Feb;
63. Mattsson N, Aisen PS, Jagust W, Mackin S, Weiner M. Brain structure and function as mediators of the effects of amyloid on memory. *Neurology*. 2015; 84:1136–44. <https://doi.org/10.1212/WNL.000000000001375> PMID: 25681451
64. Andrews KA, Modat M, Macdonald KE, Yeatman T, Cardoso MJ, Leung KK, et al. Atrophy Rates in Asymptomatic Amyloidosis: Implications for Alzheimer Prevention Trials. *PLoS One*. 2013; 8(3).
65. Mueller SG, Weiner MW. Selective effect of age, Apo e4, and Alzheimer's disease on hippocampal subfields. *Hippocampus*. 2009 Jun; 19(6):558–64. <https://doi.org/10.1002/hipo.20614> PMID: 19405132
66. Malykhin N V., Huang Y, Hrybouski S, Olsen F. Differential vulnerability of hippocampal subfields and anteroposterior hippocampal subregions in healthy cognitive aging. *Neurobiol Aging*. 2017;
67. Daugherty AM, Bender AR, Raz N, Ofen N. Age differences in hippocampal subfield volumes from childhood to late adulthood. *Hippocampus*. 2016;

68. Wisniewski HM, Sadowski M, Jakubowska-Sadowska K, Tarnawski M, Wegiel J. Diffuse, lake-like amyloid- β deposits in the parvocortical layer of the presubiculum in Alzheimer disease. *J Neuropathol Exp Neurol*. 1998;
69. Kalus P, Braak H, Braak E, Bohl J. The presubicular region in Alzheimer's disease: topography of amyloid deposits and neurofibrillary changes. *Brain Res*. 1989;
70. Murray CE, Gami-Patel P, Gkanatsiou E, Brinkman G, Portelius E, Wirths O, et al. The presubiculum is preserved from neurodegenerative changes in Alzheimer's disease. *Acta Neuropathol Commun*. 2018; 6:62. <https://doi.org/10.1186/s40478-018-0563-8> PMID: 30029687
71. Josephs KA, Murray ME, Tosakulwong N, Whitwell JL, Knopman DS, Machulda MM, et al. Tau aggregation influences cognition and hippocampal atrophy in the absence of beta-amyloid: a clinico-imaging-pathological study of primary age-related tauopathy (PART). *Acta Neuropathol*. 2017 Feb 3;
72. Crary JF, Trojanowski JQ, Schneider JA, Abisambra JF, Abner EL, Alafuzoff I, et al. Primary age-related tauopathy (PART): a common pathology associated with human aging. *Acta Neuropathol*. 2014;
73. Fiford CM, Manning EN, Bartlett JW, Cash DM, Malone IB, Ridgway GR, et al. White matter hyperintensities are associated with disproportionate progressive hippocampal atrophy. *Hippocampus*. 2017;
74. Kerchner GA. Ultra-High Field 7T MRI: A New Tool for Studying Alzheimer's Disease. *J Alzheimer's Dis*. 2011; 26(s3):91–5.
75. Carr VA, Bernstein JD, Favila SE, Rutt BK, Kerchner GA, Wagner AD. Individual differences in associative memory among older adults explained by hippocampal subfield structure and function. *Proc Natl Acad Sci*. 2017;
76. Johnson KA, Schultz A, Betensky RA, Becker JA, Sepulcre J, Rentz D, et al. Tau positron emission tomographic imaging in aging and early Alzheimer disease. *Ann Neurol*. 2016;
77. Jacobs HIL, Hedden T, Schultz AP, Sepulcre J, Perea RD, Amariglio RE, et al. Structural tract alterations predict downstream tau accumulation in amyloid-positive older individuals. *Nat Neurosci*. 2018 Feb 5;
78. Iglesias JE, Van Leemput K, Augustinack J, Insausti R, Fischl B, Reuter M, et al. Bayesian longitudinal segmentation of hippocampal substructures in brain MRI using subject-specific atlases. *Neuroimage*. 2016 Nov 1; 141:542–55. <https://doi.org/10.1016/j.neuroimage.2016.07.020> PMID: 27426838